Scientific African 24 (2024) e02233

Contents lists available at ScienceDirect

Scientific African

journal homepage: www.elsevier.com/locate/sciaf

Electrochemical detection of tryptophan in pineapple fruit using a green and chemically synthesized PANI/CuO nanocomposite modified electrode

Seleke J. Mokole [a,b], Ahmed Aliyu [c,d], Omolola E. Fayemi [a,b,*]

[a] Department of Chemistry, School of Physical and Chemical Sciences, Faculty of Natural and Agricultural Sciences, North-West University (Mafikeng Campus), Private Bag X2046, Mmabatho 2735, South Africa
[b] Material Science Innovation and Modelling (MaSIM) Research Focus Area, Faculty of Natural and Agricultural Sciences, North-West University (Mafikeng Campus), Private Bag X2046, Mmabatho 2735, South Africa
[c] Department of Chemical Engineering, Federal University Wukari, P.M.B 1020 Taraba state, Nigeria
[d] Department of Mechanical Engineering, Dalhousie University, 1360 Barrington St, Halifax, NS, B3H 4R2, Canada

ARTICLE INFO

Editor by: DR B Gyampoh

Keywords:
Tryptophan
Copper oxide nanoparticles
Polyaniline
Nanocomposites
Electrochemical detection

ABSTRACT

This study investigated the electrochemical detection of Tryptophan (Trp) in pineapple using a glassy carbon electrode (GCE) modified with nanocomposites of green and chemically synthesized copper oxide-polyaniline (PANI/CuOgrn and PANI/CuOchm). Given the properties of PANI/CuOgrn and PANI/CuOchm that have never been applied in the detection of Trp, it indicates that the development of a highly sensitive and selective sensing platform for Trp-is necessary. Such a platform would take advantage of high electric conductivity, larger surface area, and improved catalytic activity of the nanocomposites. PANI/CuOgrn and PANI/CuOchm nanocomposites were formed by doping polyaniline (PANI) with green and chemically synthesized copper oxide (CuO) nanoparticles. Using Debye-Scherrer the particle sizes of PANI/CuOgrn and PANI/CuOchm were found to be 15 nm and 13 nm, respectively. Through cyclic voltammetry (CV) and square wave voltammetry (SWV), the electrochemical behaviour of CuOch, CuOgrn, PANI/CuOchm, and PANI/CuOgrn electrodes was studied, with the focus on comparing the nanocomposites for tryptophan (Trp) catalysis. GCE-PANI/CuOchm showed a higher current response of 3.2 μA than GCE-PANI/CuOgrn. SWV was used to determine Trp, with the linear range of 5.11 μM to 25.85 μM and limit of detection (LOD) values of 3.947 and 2.037 μM for GCE-PANI/CuOchm, and 3.434 and 2.427 μM for GCE-PANI/CuOgrn. The GCE-PANI/CuOchm electrode achieved a recovered percentage of 96 % to 109 %, with an average RSD value of 18.3 (n=3), while the GCE-PANI/CuOchm electrode achieved a percentage recovery of 85 % to 103 % with an RSD value of 12.7 (n=3). The high recovery percentages for both electrodes confirm their dependability in detecting Trp. The high concentration of Trp-in the fruit and the electrode's sensitivity to identifying Trp-in actual sample analysis may account for the high recovery percentage observed.

* Corresponding author.
E-mail address: Omolola.Fayemi@nwu.ac.za (O.E. Fayemi).

https://doi.org/10.1016/j.sciaf.2024.e02233
Received 5 December 2023; Received in revised form 14 March 2024; Accepted 2 May 2024
Available online 3 May 2024

Introduction

Tryptophan (Trp) is an essential amino acid that the human body cannot synthesize and, therefore, must be obtained through consuming protein-rich foods, such as nuts, milk, fish, bananas, and cheese [1,2]. Trp-is a precursor for the neurohormone melatonin, which is crucial in regulating the sleep-wake cycle and promoting sleep [3]. It is also a precursor for serotonin, a neurotransmitter that regulates sleep and impacts mood, hunger, and pain [4,5]. Additionally, Trp-helps maintain the body's nitrogen balance and supports healthy body weight and muscle mass [6,7]. The World Health Organization (WHO) recommends that Trp-intake should not exceed 4 mg/kg per day, which is also contingent on body weight [6]. When the body fails to process or metabolize Trp-correctly, it may result in the generation of toxic substances that trigger crises such as schizophrenia, hallucinations, and delusions [2]. A Trp-deficiency can lead to severe mental illnesses such as anxiety and depression by depleting serotonin and causing melatonin depletion, resulting in sleeplessness. Excessive Trp-consumption can be just as harmful to human health as Trp-deprivation, causing a range of gastrointestinal issues, including nausea, stomach discomfort, diarrhea, lack of appetite, and sexual dysfunction [1,8].

Various methods have been employed to detect Trp, including chromatography techniques like ultra-high performance liquid chromatography with electrospray ionization, microscopic techniques such as cryoelectron microscopy, and spectroscopic techniques like fluorescence microscopy-mass spectroscopy with a triple quadrupole [8]. However, electrochemical sensors face challenges when detecting Trp. For example, the bare electrode may foul when other molecules such as ascorbic acid (AA) and dopamine (DA) are detected alongside Trp, resulting in overpotential. Furthermore, Trp's electron transfer process is slow, and its electrochemical activity is poor [9].

Nanotechnology, a technical discipline used in nanoscience to build and use functional structures measured in nanometers, offers several synthesis methods, including chemical and green synthesis. Green synthesis, which utilizes enzymes, microbes, plants, fungi, and plant extracts, is an ecologically benign approach due to its efficient use of less toxic solvents and its ability to maximize production while minimizing the harmful by-products of numerous chemical processes [10,11]. Despite its drawbacks, the chemical method produces goods through planned chemical processes; it is believed to be repeatable, reliable, and efficient enough to be employed in numerous laboratories [11-13].

Both chemically synthesized and green synthesized copper oxide (CuO) nanoparticles (NPs) offer several benefits, including the capacity to be used in a wide range of applications. CuO NPs are used in rocket propellants as burning catalysts, lowering the index pressure and improving the homogenous propellant burning rate; they are helpful in energy storage due to their high redox behavior, tiny band gap with optimized shape, and low dielectric constant. CuONPs are also used as ceramic resistors due to their high electric resistance, high temperature stability, and low thermal expansion coefficient. Similarly, polyaniline (PANI) has several uses since it is the best polymer in the family of inherently conducting polymers. It is highly respected because of its electrical qualities, which can be tuned, have a low cost, and have other significant characteristics [14-19]. PANI is used in EMI shielding due to its resistance to mechanical and thermal stress and high dielectric constant, allowing electromagnetic waves to be conducted away from the shielded device. Due to PANI's resistance to corrosion and heat and high breakdown voltage, which allows it to withstand high electric fields without breaking, it is used in electric discharge systems. When both CuO NPs and PANI are used in electrochemical sensors as a mixed CuO/PANI nanocomposite, the polymers toughness, flexibility, and coat-ability improve. Furthermore, the metal oxides endurance and hardness will improve, making the nanocomposite superior to the polymer and metal oxide separately [15-20]. PANI/CuO nanocomposite has anti-corrosive and EMI shielding due to the synergistic effect of both PANI and CuONPs, and this makes them suitable for applications in electromagnetic shielding and electronic devices. The composite can be used in a variety of industries, including aerospace, automotive, and marine [14].

Other materials have been used for the detection of Trp, which have shown to have very low detection limits such as Pd-Cu@Cu_2O/N-RGO [21], boron-doped diamond nanowires [22], and flower-like cerium vanadate microstructures [23] and had LOD's of 1.9 nm, 0.5 μM, and 0.024 μM, but PANI/CuO has never been used for the detection of Trp-in literature. This study presents the electrochemical detection of Trp-in pineapple fruits, as well as Trp-in the presence of other molecules such as ascorbic acid (AA) acid and dopamine (DA), by using green and chemically synthesized PANI/CuO nanocomposites with the intention of comparing their electrochemical properties such as catalytic activity, redox, which are affected by surface area and surface energy, conductivity, which are fundamental properties required in an electrochemical sensor, and also to observe which one of the green and chemically synthesized materials has better sensitivity and selectivity so that they can be applied in sensors even. Cyclic voltammetry (CV) and square wave voltammetry (SWV) were used to conduct the study between green and chemically synthesized nanocomposites. The GCE-PANI/CuO_{chm} modified electrode demonstrated superior electrocatalytic and electroanalytic properties for detecting Trp-compared to the GCE- PANI/CuO_{grn} modified electrode.

Materials and methods

Materials

Ziziphus mucronata, a plant species indigenous to South Africa, is utilized to greenly synthesize CuO through the utilization of its dried leaves. Copper (II) nitrate trihydrate (Cu(NO3)2·3H2O) (90 %), dopamine hydrochloride (98 %), ethylene glycol (99.5 %), aniline hydrochloride (99 %), hydrochloric acid (HCl) (32 %), ammonium peroxydisulphate ((NH4)2S2O8) (98 %), sodium hydroxide (NaOH) (98 %), potassium hexacynoferrate (IV) (K4[Fe(CN)6]) (99 %), potassium hexacynoferrate (III) (K3[Fe(CN)6]) (99 %) and N, N-Dimethylformamide (DMF) (USA) (99 %) were utilized with exactitude in their analytical-grade form, without requiring further purification. The preparation of all solutions involved the use of distilled water that had been deionized (DI).

Preparation of PANI/CuO nanoparticles

In a prior study [16], a thorough investigation was conducted on the synthesis and characterization of CuO nanoparticles produced through both chemical and green methods. Additionally, using a ratio of 1:1 for green and chemically synthesized nanoparticles and PANI, 3 ml of DMF was added to the individual vials. The vials were sonicated for 24 hours at 25 ℃ to create a PANI/CuO nanocomposite paste [16].

pH optimization

pH optimization was done at GCE-PANI/CuO at various pH (pH 3, pH 6, pH 7, and pH 9) and was repeated at pH 7.0 to 7.9 after discovering that pH 7 has the highest current response in 0.1 M PB solution containing 0.1 mM Trp-at 25 mV/s scan rate. This study is important since Trp, AA, and DA are present in blood at a physiological pH of 7.4 [24].

Electrocatalysis

Autolab's electrochemical experiments utilized a glassy carbon electrode (GCE) as one of its electrodes. The electrode was carefully prepared for experimentation by initially cleaning it using a mixture of aluminum oxide (Al_2O_3) and distilled water. The cleaning surface was subjected to an infinity sign drawn with an Al_2O_3 mixture. The electrode was then submerged in distilled water and sonicated for 5 minutes, followed by submersion in ethanol for another 5 minutes, and then returned to distilled water for 5 minutes. Subsequently, the electrode was dried at 50 °C for 5 minutes before being modified with nanomaterials through drop-drying and then dried again for an additional 5 minutes.

The electrochemical cell in use utilized three electrodes - a reference, counter, and working electrode. The cyclic voltammetric method was employed to perform the electrocatalytic experiment with DA, AA, and Trp. The experiment used potential ranges of -0.4 V and 1.2 V for Trp, with a scan rate of 25 mV/s. The anodic (Ipa) and cathodic (Ipc) peak currents, formal redox potential (E^o), and peak separations (ΔE) were all carefully examined parameters.

Concentration study

To investigate concentration levels, the GCE electrode was coated with PANI/CuO_{grn} and PANI/CuO_{chm} nanocomposites and subjected to square-wave voltammetry (SWV). The SWV method utilized a potential window range of -0.4 to 1.2 V, a frequency of 10 Hz, a potential amplitude of 0.01 V, and an Estep for potential amplitude (0.01). By measuring the produced concentrations, the electrode's sensitivity towards the analyte (Trp) was determined, along with the limit of detection (LOD) and limit of quantitation (LOQ).

Preparation of real sample analysis

First, 5 g of pineapple fruit were weighed and blended using a blender machine. Then, 100 ml of PB solution with a pH of 7.4 were added, and the mixture was swirled for 10 minutes. To obtain the supernatant, a centrifuge was used for 15 min at 4430 rpm to separate the resulting mixture. Different concentrations of Trp-were added to the pineapple extract. The GCE- PANI/CuO_{grn} and PANI/

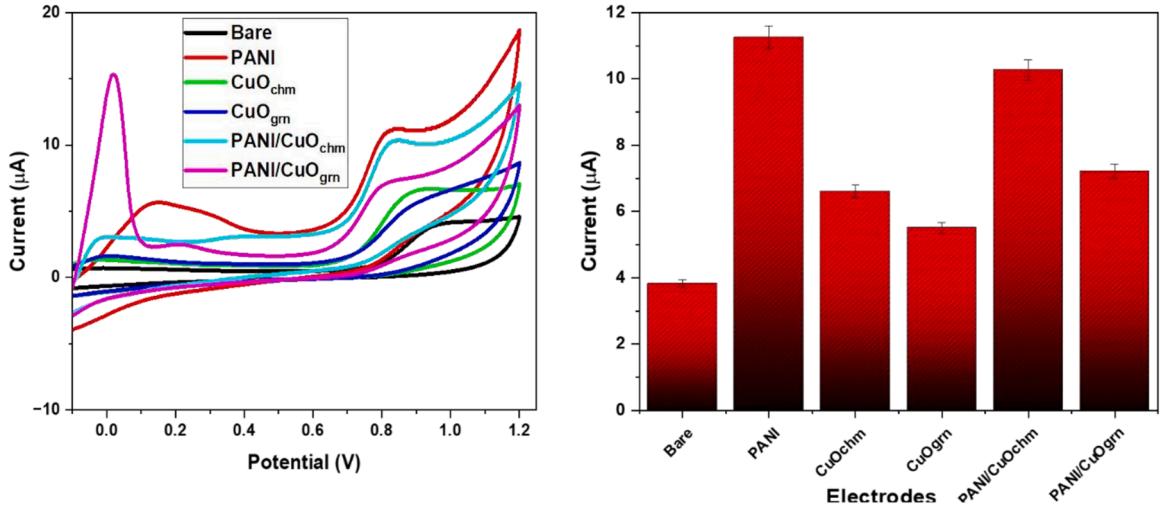

Fig. 1. Comparative cyclic voltammogram of unmodified and modified electrodes in Trp-probe in 0.4 mM PB (pH 7.4), 1(b) Current response of all the electrodes.

CuO_{chm} electrodes were utilized to quantify Trp-concentration quickly in spiked and un-spiked samples [16].

Results and discussion

Electrocatalysis of Trp

The electrocatalytic behavior of unmodified, green, and chemically modified electrodes towards the oxidation of Trp-is presented in Fig. 1(a) through cyclic voltammetric responses. The GCE-bare, GCE-PANI, GCE-CuO_{grn}, GCE-PANI/CuO_{grn}, GCE-CuO_{chm}, and GCE-PANI/CuO_{chm} electrodes were utilized in a Trp-probe produced in 0.4 mM pH 7 PB solution within a potential window of -0.4 to 1.3 V at 25 mV/s scan rate. Using Debye-Scherrer the particle sizes of PANI/CuO_{grn} and PANI/CuO_{chm} were found to be 15 nm and 13 nm, respectively. Fig. 1(a) indicates that the CV of Trp-has two oxidation potentials; the first one was found around 0.01 V, which is for Trp-radical cation, and the second oxidation peak was found at 0.8, which is for 3- hydroxykynurenine. The synergistic effect of combining PANI and CuONP's is the reason for the presence of two oxidation peaks, which improved the catalytic activity and electron transfer kinetics of all the electrodes and facilitated the various oxidation stages of Trp [19,25]. The combination of the excellent properties of PANI and CuOchm provides the nanocomposite with a surface area with an electron transfer microenvironment, enabling the sensitive determination of Trp. All the electrodes have an oxidation peak with no reduction peak, indicating an irreversible reaction resulting from the redox-active indole group of Trp, which undergoes two-electron reduction during cyclic voltammetry. The first electron reduction occurs in the indole ring, resulting in unstable products, which is the Trp-radical cation, which reacts further, forming irreversible stable products that cannot be oxidized back to Trp, and the second one occurs at the amino side chain [25]. The mechanism of Trp-involves the formation of Trp-radical cation by abstraction of an electron, followed by the C2 rearrangement of the radical species, which undergoes hydroxylation, forming a carbon-centered radical, which undergoes intermolecular cyclization, forming 3-hydroxykynurenine [25,26].

Among the different electrodes tested, GCE-PANI exhibited the highest current response, suggesting superior electroanalytical properties. PANI usually shows a shuttle shape at a pH greater than 7 due to the absence of anions. However, in this case, it displayed a normal peak, which is a result of the presence of ions in the phosphate buffer solution. The ions caused PANI to undergo an exchange reaction, whereby protons in the polymer are replaced by anions, and this is called the ion exchange phenomenon, leading to PANI showing a normal peak at a pH greater than 7 instead of the shuttle-shaped peak. Additionally, the proton replacement in the polymer increases the mobility of the charge carriers. This is widely used in pH sensors [27]. GCE-PANI/CuOchm demonstrated a high current response and had the second-highest oxidation peak compared to other electrodes. This may indicate that GCE-PANI/CuOchm possesses superior catalytic properties and a larger surface area, resulting from the presence of PANI. This, in turn, enhances its conductivity and electron transfer acceleration capacity. Additionally, CuO's properties, such as its smaller bandgap than PANI and its high adsorption capacity, may have contributed to GCE-PANI/CuOchm's improved conductivity and sensing performance. These findings are supported by a previous study [16]. The order of current response and electron transfer is represented in Fig. 1(b), with GCE-PANI (11.12 μA) exhibiting the highest response followed by GCE-PANI/CuOchm (10.34 μA) > GCE-CuOchm (8.93 μA) > GCE-PANI/CuOgrn (7.14 μA) > GCE-CuOgrn (5.76 μA) > GCE-Bare (3.88 μA). The Epa for all modified electrodes was consistent with the literature [21], ranging from 0.8 to 0.9.

Electrochemical impedance spectroscopy in 0.4 mM Trp

Electrochemical impedance spectroscopy (EIS) was used to investigate the electron transport properties of both modified and unmodified electrodes. To conduct the EIS experiment, we used five different electrode coating materials in a 0.4 mM Trp-solution

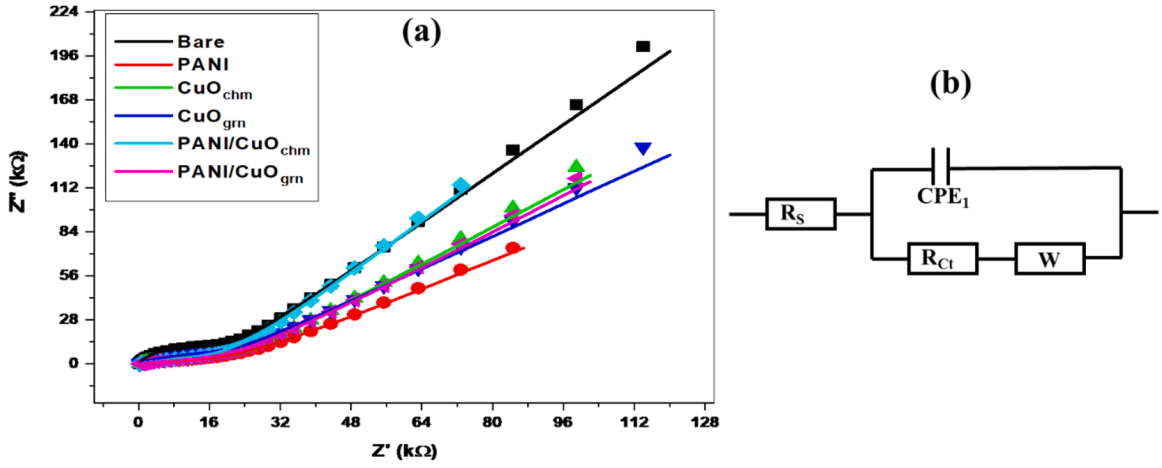

Fig. 2. **(a)** Fitted Nyquist plot for modified and unmodified electrodes, (b) typical EIS fitting circuit for modified and unmodified electrodes.

prepared in 0.1 mM PB with a pH of 7.4. The experiment was carried out using Autolab with a frequency set ranging from 100 kHz to 0.1 Hz and a fixed potential of 0.2 V. The Nyquist plot fitted of all the modified and unmodified electrodes is represented in Fig. 2(a). The R_{ct} values were 21.54 kΩ < 14.75 kΩ < 12.59 kΩ < 12.48 kΩ < 9.79 kΩ < 9.56 kΩ for GCE-Bare, GCE-CuO_{grn}, GCE-PANI/CuO_{grn}, GCE-PANI/CuOchm, GCE-PANI, and GCE-CuOchm, respectively. Our results indicated that the electrode modification for all the modified electrodes was successful.

Table 1 indicates that all electrodes, except for GCE-CuOchm, exhibited matching CV data for both modified and unmodified electrodes at 0.4 mM Trp. The unstable behavior of GCE-CuOchm may be attributed to the high surface reactivity of CuO. This reactivity often triggers reactions with surrounding electrolytes, leading to changes in surface properties and the formation of hydroxide and copper species (CuO or Cu_2O), which ultimately affect electrode stability and reproducibility. Additionally, CuO may undergo a redox reaction, altering its oxidation state and disrupting the electrode-electrolyte charge transfer interface. Another potential factor contributing to the unstable behavior of GCE-CuO_{chm} is the adsorption of Trp-to the electrode surface, which varies due to surface charge and roughness and may introduce measurement variability and instability [24,28,29]. Additionally, there were slight deviations between the curve for bare electrodes and modified electrodes, particularly in the high-frequency region. This is likely due to the surface modification of the bare electrode with nanocomposites, which increases the surface area and affects the electrode-electrolyte interface, leading to a slight deviation in impedance curves. Fig. 2(b) depicts the typical circuit used to fit all electrodes, and Table 2 outlines the circuit components, with Rs indicating solution resistance, Rct representing charge transfer resistance, CPE denoting the constant phase element, and χ^2 representing the Chai-square value [30].

Effects of scan rate on the electrocatalysis oxidation of Trp at the GCE-PANI/CuO_{grn} and GCE-PANI/CuO_{chm} electrodes

The effect of the scan rate on GCE-PANI/CuOgrn and GCE-PANI/CuOchm electrodes with a 0.4 mM Trp-concentration, utilizing CV techniques, was examined. The corresponding CV response is presented in Fig. 3(a) and 4(a) for GCE-PANI/CuOgrn and GCE-PANI/CuOchm electrodes, respectively. Fig. 3(a) illustrates the presence of two distinct oxidation peaks for Trp-radical cation and an additional peak for 3-hydroxykyurenine. A single reduction peak is observed, which is attributed to Trp-radical cation, an intermediate species that is unstable and, therefore, undergoes reduction to form 3-hydroxykynurenine. The latter is a highly stable product with limited potential for further reduction and hence exhibits a single oxidation peak.

Fig. 3(b) illustrates the I_{pa}/I_{pc} regression plot against the square root of the scan rate. The relationship between the peak current and scan rate was found to be proportionally correlated with the scan rate. The oxidation of Trp's phenyl ring and Trp's function as a reducing agent at the electrode surface was observed in the GCE-PANI/CuOchm electrode. The increase in peak potential with the 25 to 500 mV increase of the scan rate indicated that an adsorption-controlled reaction took place. The anodic reaction was represented by Ipa = 0.3596 + 0.2467 v1/2 with R2 = 0.999, and the cathodic reaction was represented by Ipc = – 0.3180 – 0.1897 v1/2 with R^2 = 0.9918. Both Fig. 3(b) and (c) demonstrated that current and scan rates were directly related and increased linearly. The equations for anodic and cathodic peak currents in Fig 3(c) were Ipa = 1.4408 + 0.0664 v (R2 = 0.998) and Ipc = –1.1384 – 0.0392 v (R2 = 0.996), respectively. The Tafel value for this curve was determined to be 410.6 mV/dec, which was more than 118 mV/dec. This suggests that adsorption occurred at the electrode surface due to oxidation products or the participation of chemical intermediates [39]. The Randles-Sevcik equation [39] was used to describe the relationship between peak current (I_p), square root of scan rate ($v^{1/2}$), and scan rate (v) for both Fig. 3(b) and (c) and Fig. 4(b) and (c).

$$I_p = 2.69 \times 10^5 \, n^{\frac{3}{2}} A D^{\frac{1}{2}} C \nu^{\frac{1}{2}} \quad (1)$$

Where I_p represents the anodic peak current (A), n is the number of electrons transferred, *A* is the effective electroactive surface area (cm^2), C is the constant concentration of Trp (mol cm^{-3}), *D* is the diffusion coefficient (cm^2 s^{-1}), and *ν* is the scan rate (v s^{-1}).

In contrast, in Fig. 4(a), the GCE-PANI/CuOgrn electrode displayed an oxidation peak without a reduction peak, indicating that the Trp-underwent an irreversible oxidation reaction at the electrode surface. Trp-was oxidized to its corresponding products, which were not reduced back during the reverse scan, likely due to the catalyst PANI/CuOgrn, which favored the oxidation of Trp-and inhibited its reduction. The roughness and surface charges of the modified electrode surface were potential factors that may have affected the electrochemical properties of Trp [40,41]. Fig 4(b) shows the I_{pa}/I_{pc} regression plot versus the square root of the scan rate, illustrating that the peak current and scan rate were proportionally correlated by the scan rate. The GCE-PANI/CuO_{grn} electrode oxidized Trp's phenyl ring, while Trp-acted as a reducing agent at the electrode surface. The steady increase in peak potential with the 25 to 500 mV increase in the scan rate demonstrated this [42]. The anodic equation from Fig. 4(b) is Ipa = 0.3180 + 0.18975 v1/2 with R2 = 0.997, indicating that the reaction was adsorption controlled. Fig 4(c) shows that the current versus scan rate grew linearly with equations Ipa

Table 1
CV data obtained at different unmodified and modified electrodes.

Elements	Ipa (μA)	Ipc (μA)	Ipa/Ipc	Epa (V)	Epc (V)	E^o (V)	ΔE (V)
GCE-bare	4.11	–	4.11	0.99	–	0.99	0.49
GCE-PANI	11.15	–	11.15	0.82	–	0.82	0.41
$^{GCE\text{-}CuO}$chm	6.66	–	6.66	0.93	–	0.93	0.46
$^{GCE\text{-}CuOgrn}$	5.89	–	5.89	0.91	–	0.91	0.45
GCE-$^{PANI/CuO}$chm	10.33	–	10.33	0.84	–	0.84	0.42
$^{GCE\text{-}PANI/CuO}$grn	7.19	–	7.19	0.82	–	0.82	0.41

Table 2
Fitted EIS parameters of all the electrodes in Trp.

Elements	Rs (kΩ cm^2)	Rct (kΩ cm^2)	CPE1 (μF/cm^2)	W (μS $s^{0.5}$/cm^2)	χ^2
GCE-bare	0.184 (2.99)	21.54 (2.10)	0.32 (1.20)	5.92 (1.65)	0.00038529
GCE-PANI	0.186 (2.00)	9.79 (5.41)	5.16 (1.56)	13.28 (2.98)	0.00058899
GCE-CuOchm	0.180 (2.52)	9.56 (3.62)	1.56 (1.61)	9.38 (2.19)	0.00058782
GCE-CuOgrn	0.194 (2.96)	14.75 (3.55)	0.90 (1.68)	8.44 (2.41)	0.00070901
GCE-PANI/CuOchm	0.180 (1.49)	12.48 (4.58)	3.61 (1.02)	8.17 (2.03)	0.00027717
GCE-PANI/CuOgrn	0.185 (2.82)	12.59 (7.61)	3.25 (2.03)	8.24 (3.83)	0.0001064

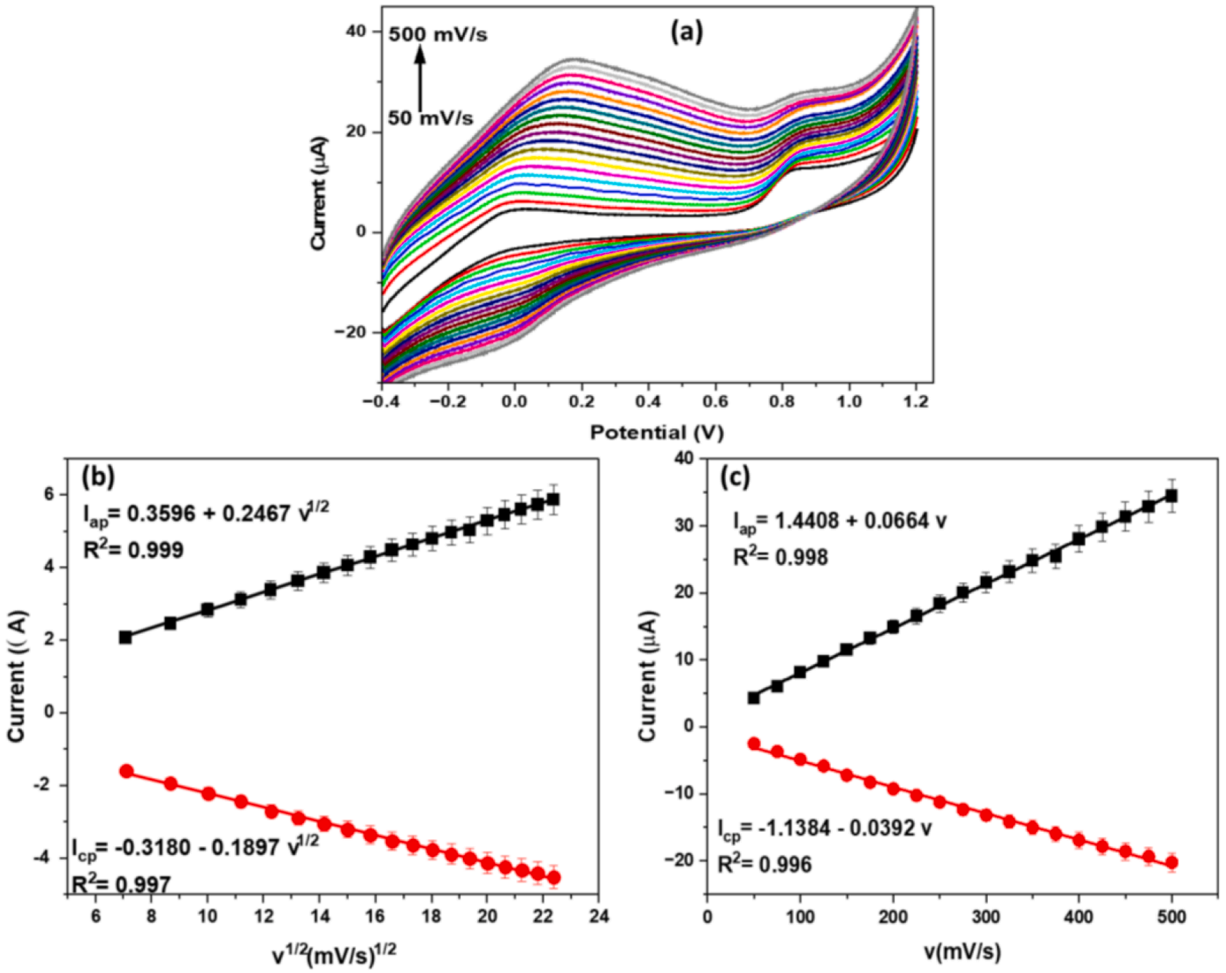

Fig. 3. (a) Scan rate of GCE-PANI/CuO_{chm} modified electrode (b) Ipa/Ipc regression plot vs. square root of scan rate, and (c) regression plot of current vs. scan rate in 0.4 mM Trp-prepared in 0.1 mM PB (pH 7.4).

= 1.1384 + 0.0392 v (R2 = 0.996), illustrating that as the current increases, so does the scan rate. Therefore, both the GCE-PANI/CuOchm and GCE-PANI/CuOgrn composites exhibited adsorption control at the electrode surface.

Concentration studies of Trp using GCE-PANI/CuO_{grn} and GCE-PANI/CuO_{chm} electrodes

The present study investigates the square wave voltammograms (SVW) recorded at GCE- PANI/CuO_{chm} over the range of 5.11 μM to 28.85 μM of Trp-concentration as shown in Fig. 5(a). The linear plot of reduction current peaks against Trp-concentration produced in 0.1 mM of 7.4 pH PB solution is presented in Fig. 5(b). The potential window was adjusted at 0.5 to 1.2 V, with a frequency of 10 Hz, an amplitude of 0.01 V, and a potential step of 0.01 V.

The study reveals that the peak current decreased as the concentration of Trp-increased, indicating an inversely proportional relationship between the two. This is attributed to the fact that as the concentration increases, the rate of reaction at the electrode

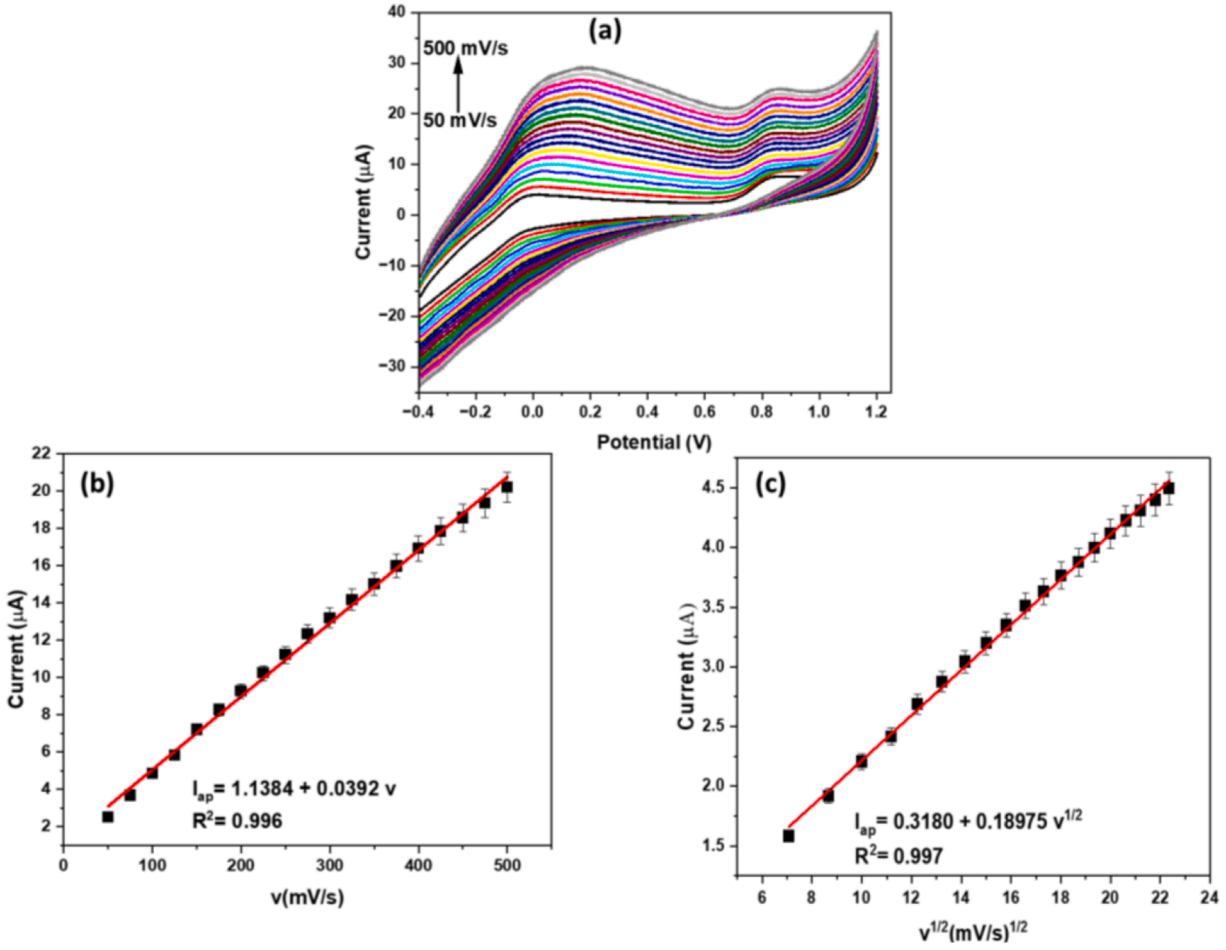

Fig. 4. (a) Scan rate of GCE-PANI/CuOgrn modified electrode (b) Ipa/Ipc regression plot vs. square root of scan rate, and (c) regression plot of current vs. scan rate in 0.4 mM Trp-prepared in 0.1 mM PB (pH 7.4).

surface increases. However, the mass transport rate cannot keep up with the increased reaction rate, and the concentration of the Trp-at the electrode surface decreases. Consequently, a lower current response is observed even though the concentration of Trp-is increased [43]. Since there are two peaks belonging to the Trp-molecule, the linear equations were I = 67.084 – 1.01522 [Trp] and I = 14.877 - 0.0975 [Trp], and the regression score were $R^2 = 0.989$ and $R^2 = 0.993$ for Trp-radical cation and 3-hydroxykynurenine, respectively. Using Eqs. (1) and (2), LOD was estimated to be 3.947 and 2.037 μM, and the LOQ to be 11.960 and 6.171 μM, respectively.

$$\mathrm{LOD} = \frac{3.3 \times \textit{standard deviation}}{\textit{Slope}} \tag{2}$$

$$\mathrm{LOQ} = \frac{10 \times \textit{Standard deviation}}{\textit{Slope}} \tag{3}$$

The findings of the SWV at the GCE-PANI/CuOgrn nanocomposite-modified electrode, at various tryptophan (Trp) concentrations, are presented in Fig. 6(a). The corresponding linear plot of reduction current peaks versus Trp-concentrations prepared in 0.1 mM PB (pH 7.4) is shown in Fig. 6(b). The Trp-concentrations tested ranged between 4.7 μM and 24.35 μM, and the results of Fig. 6(b) indicate that there was a linear proportionate relationship between the peak current and the changing concentrations. This relationship demonstrates that as the Trp-concentration increased, so did the peak current. The linear regression equation for Trp-radical cation and 3-hydroxykynurenine, respectively, were I = 108.7737 – 0.6165 [Trp] ($R^2 = 0.961$) and I = 21.72331 + 0.25128 [Trp] ($R^2 = 0.990$). The limits of detection (LODs) were 3.434 μM and 2.427 μM, and the limits of quantification (LOQs) were 10.409 μM and 7.354 μM, respectively. These values were higher than those of GCE-PANI/CuOchm, indicating that GCE-PANI/CuOchm was a better-modified electrode due to its lower detection limit and greater sensitivity for Trp-detection than GCE-PANI/CuOgrn. However, GCE-PANI/CuOgrn managed to detect Trp-at a slightly smaller concentration than GCE-PANI/CuOchm, which explains the smaller differences in the linear range concentrations. Both electrodes showed great sensitivity in detecting Trp, but both also had LODs (limits of

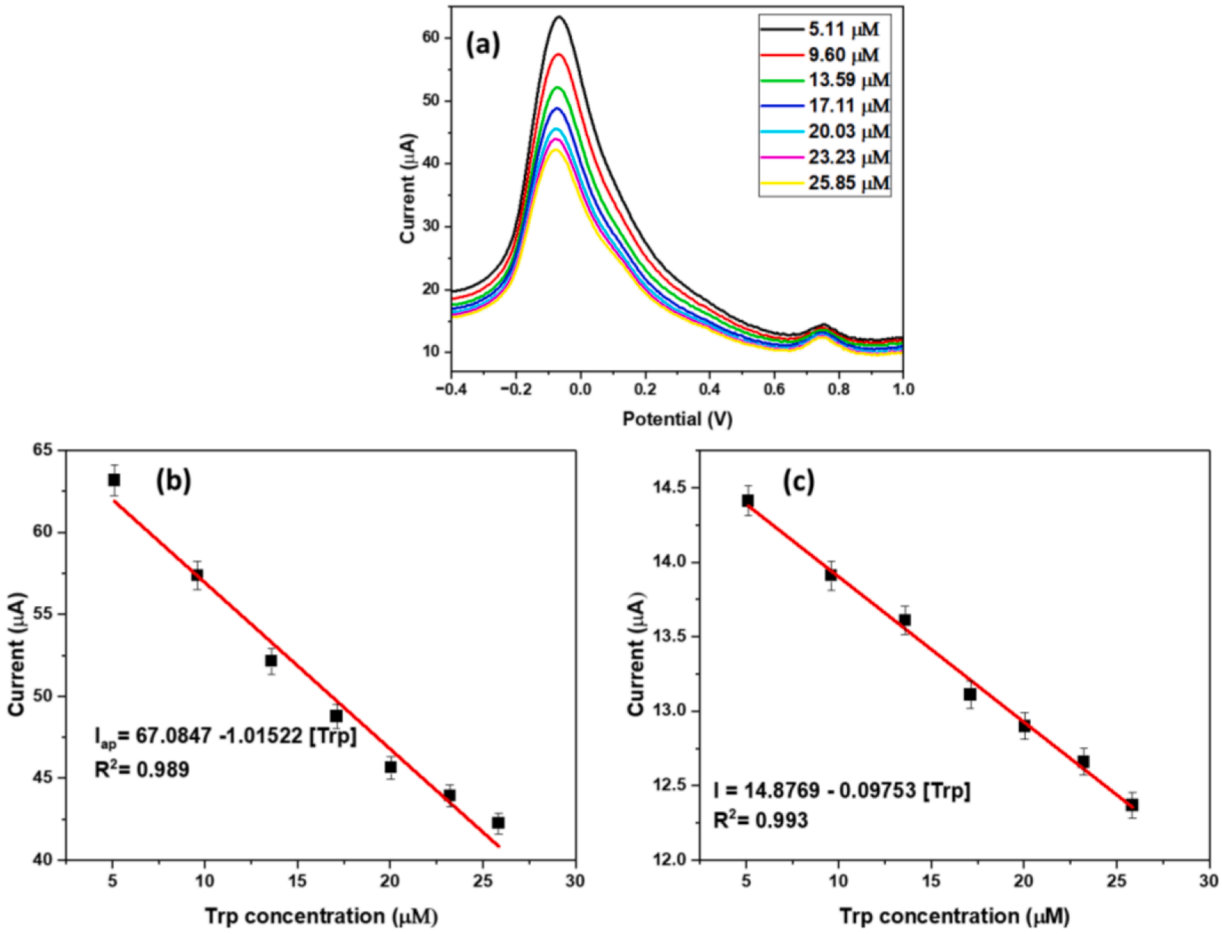

Fig. 5. (a) SVW recorded at GCE-PANI/CuOchm electrode over the Trp-concentration range of 5.11 µM to 25.58 µM, and (b) plot of peak currents versus concentrations of Trp.

detection) outside of their linear range. This could be due to the saturation of the electrode surface, which was observed in the case of GCE-PANI/CuO_{chm}, which was experiencing a mass transfer peak current limit. This limit is related to the diffusion coefficient of the analyte and can affect the sensitivity of the system, thus affecting the linear range [31]. PANI/CuO nanomaterials were experiencing saturation at the electrode surface, which explains why both had LODs outside of their linear range. Table 3 shows that the reported sensors are well comparable with reported sensors in the literature.

Interference studies: simultaneous detection of Trp, DA, and AA using GCE-PANI/CuO_{grn} and GCE-PANI/CuO_{chm} modified electrodes

This study examined the feasibility of using green and chemically modified electrodes to separate Trp-from interfering substances such as DA and AA. The reason for using DA and AA is due to the presence of the Trp-radical cation peak at 0.01 V on CV, which DA and AA could easily interfere with. DA in this paper is used to determine whether the modified electrode will be able to be sensitive enough to differentiate between the Trp-radical cation peak and those of DA and AA, which are very close potential on CV. To achieve this, square wave voltammetry was utilized to simultaneously detect the presence of AA, DA, and Trp. The concentrations of AA and DA were held constant at 0.4 mM, while Trp-concentrations were raised from 66.7 to 164.7 µM. In Fig. 7(a), for the PANI/CuOchm electrode, three distinct peaks were observed at -0.05, 0.23, and 0.8 V, which corresponded to AA, DA, and Trp, respectively. On the other hand, for GCE-PANI/CuOgrn electrode (Fig. 8(c)), peaks were observed at -0.05, 0.22, and 0.80 V for AA, DA, and Trp, respectively. Both nanomaterials showed selectivity for Trp-because of the presence of the benzene ring and carboxyl group in their structure, which DA and AA do not have, which allowed for the formation of π-π interaction with PANI in the composites. In both Fig. 7 (a) and 8(a), the peak attributed to AA replaced that of the Trp-radical cation, as AA has a higher standard reduction potential of +0.23 V than that of Trp-radical cation (+0.80 V). This indicates that AA can be oxidized more easily than Trp-radical cation and thus can be oxidized at a lower potential, leading to a shift in the peak. The selectivity of PANI/CuO nanocomposite towards Trp-is due to the chemical structure of Trp-and the high density of catalytically active sites on the surface of PANI/CuO nanocomposite that resulted from the synergetic impact of the composite [44]. PANI/CuO nanocomposite reacted specifically with Trp-via a mechanism called

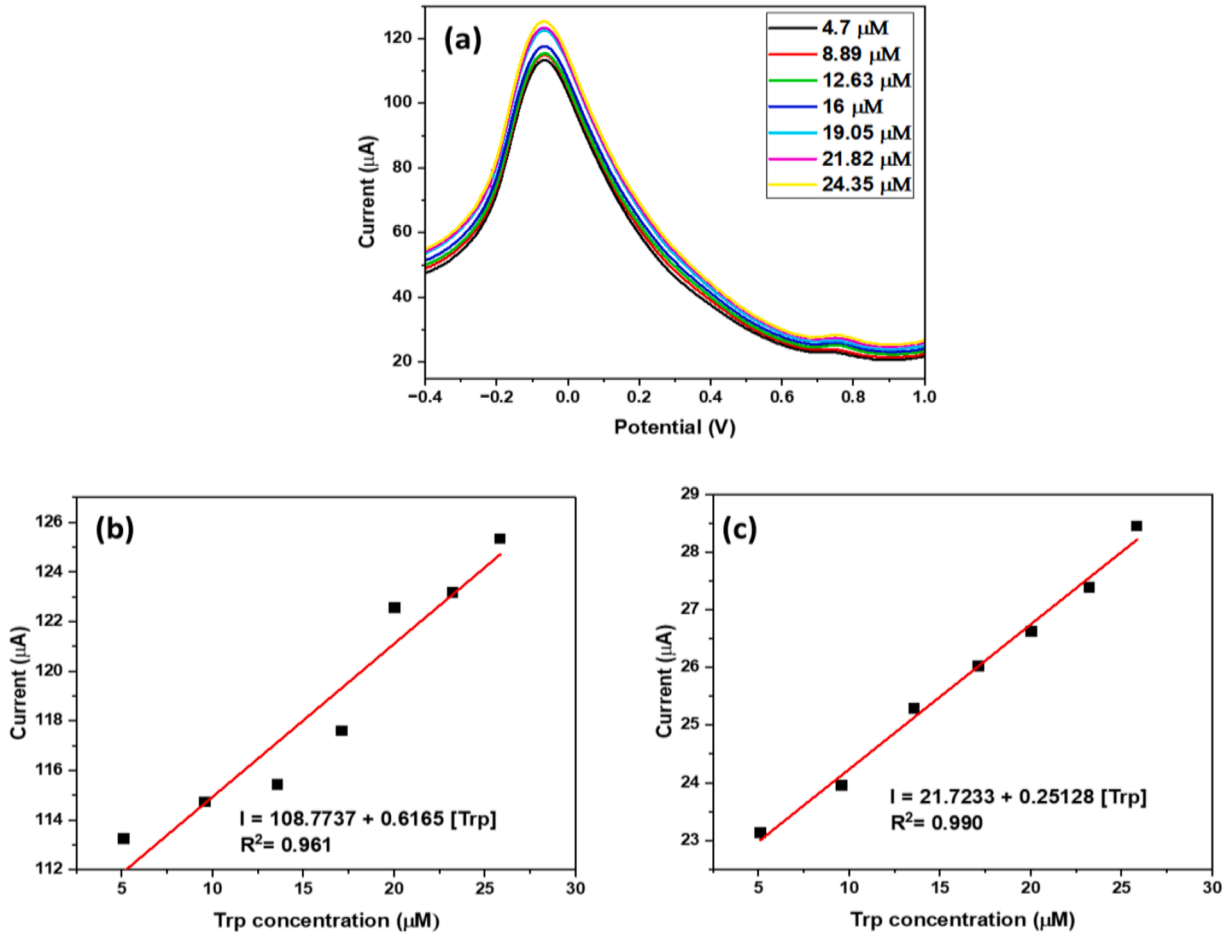

Fig. 6. (a) SVW recorded at GCE-PANI/CuOgrn electrode over the Trp-concentration range of 4.7 µM to 24.35 µM, and (b) plot of peak currents versus concentrations of Trp.

Table 3
A comparison of previous sensors works with the present study.

Elements	LOD (µM)	Linear range (µM)	Technique	References
PT-CuO	0.015	0.100 – 0.001	CV	[31]
CPE-ZrO_2/CuO/CeO_2	7.2	8.6 – 194	DPV and CV	[32]
GCE-$MnWO_4$/RGO	0.0044	0.001 – 120	DPV and CV	[33]
Co-Ni-MOFs/$^{GCE/p\text{-}ARG}$	0.3	1.0 – 7.0	SWV	[34]
Graphite electrode	1.73	5.0 – 150	CV and DPV	[35]
Cs/Ce-MOF	0.14	0.25 – 331	DPV	[36]
2D/2D porous Co3O4/rGO	0.26	1.0 – 800	CV and LSV	[37]
GCE/ZnO	1.49 and 0.94	–	CV and LSV	[38]
GCE-PANI/CuOchm	3.9 and 2.0	5.11 -25.85	SWV	This work
GCE-PANI/CuOgrn	3.4 and 2.4	4.7 – 24.35	SWV	This work

surface-assisted L-Trp-oxidation, whereby the highly reactive surface area allowed for a large number of Trp-and the high reactivity of CuONP's ensured the rapid oxidation of Trp [6], while the PANI matrix was stabilizing CuONP's and improving the selectivity for Trp.

The observed peaks in Fig. 7(a) and (c) decreased linearly with increasing concentration, and this was confirmed by the plot of current versus concentrations in Fig. 7(b), which demonstrated an inverse relationship between concentration and current. In this study, both electrodes showed strong anti-interference capabilities, displaying three distinct and sharp peaks at different potentials corresponding to different molecules based on the existing literature [45,46].

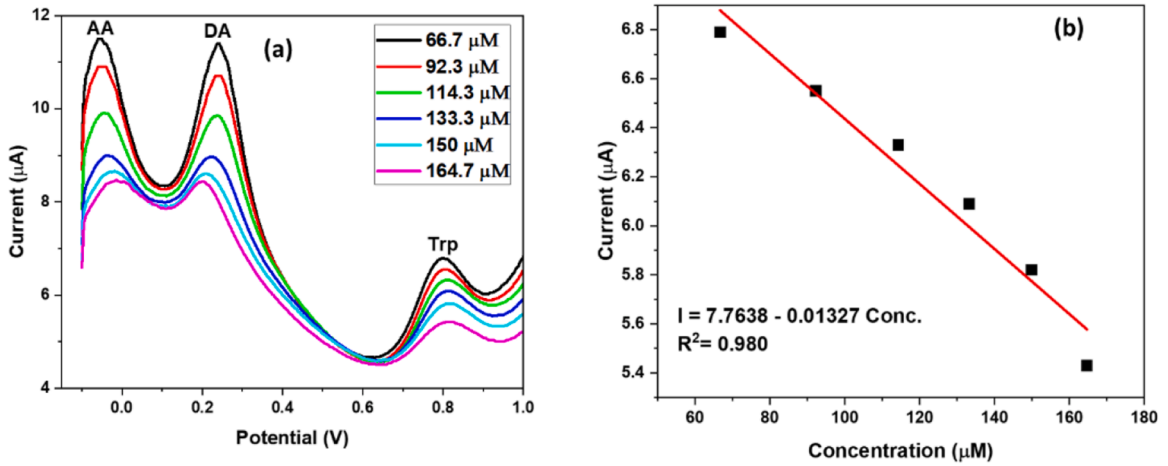

Fig. 7. SVW of (a) GCE-PANI/CuOchm in 0.4 mM of AA, DA and Trp-prepared in pH 7 PB solution of 0.1 mM, and (b) plot of peak currents versus concentrations of Trp.

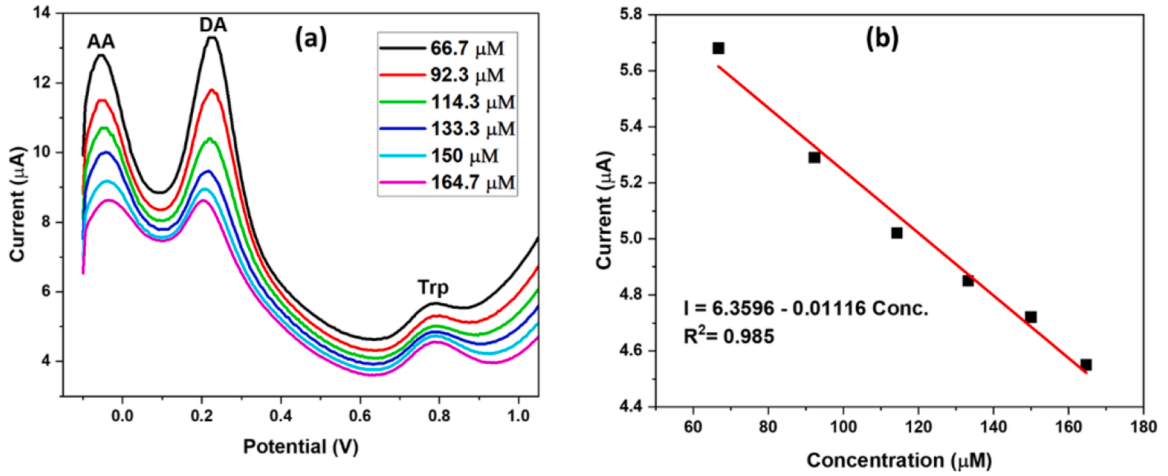

Fig. 8. SVW of (a) GCE-PANI/CuOgrn in 0.4 mM of AA, DA and Trp-prepared in pH 7 PB solution of 0.1 mM, and (b) plot of peak currents versus concentrations of Trp.

Real sample analysis

This investigation aimed to evaluate the sensors' ability in food samples. Using SWV, Trp-detection in pineapple was achieved using GCE-PANI/CuOgrn and GCE- PANI/CuOchm electrodes. The findings, outlined in Table 4, reveal that the GCE-PANI/CuOgrn electrode exhibited an RSD value of 12.7 (n=3) with recovery percentages ranging from 85 to 103 %, whereas the GCE-PANI/CuOchm electrode had a recovery percentage of 96 to 109 % with an RSD value of 18.3 (n=3). The high recovery percentages obtained from both electrodes affirm their reliability in detecting Trp. These high recovery values could be attributed to the high concentration of Trp-in the fruit and the electrodes' sensitivity to Trp-detection during sample analysis.

Conclusion

The present study reports the successful synthesis of green and chemical PANI/CuO nanocomposites. The electrocatalytic activity, selectivity, and current response of both GCE- PANI/CuOgrn and GCE-PANI/CuOchm were found to be robust. The SWV technique was employed to detect Trp, and the linear range of detection was 147 µM to 217 µM. The GCE-PANI/CuOgrn electrode exhibited an LOD of 3.434 and 2.427 µM, while the GCE- PANI/CuOchm electrode showed an LOD of 3.947 and 2.037 µM. Both green and chemical nanocomposites Real sample analysis was performed using pineapple fruit, and the GCE-PANI/CuOgrn electrode presented recovery percentages ranging from 85 to 103 % with an average RSD value of 17.0 (n=3). On the other hand, the GCE-PANI/CuOchm electrode showed recovery percentages ranging from 96 to 109 % with an RSD value of 5.4 (n=3). Notably, our results suggest that GCE-PANI/

Table 4
Trp-recovery from pineapple fruit.

Sample	Added (μM)	Detected (μM)	Recovery (%)	RSD (%)
GCE-PANI/CuOchm Electrode				
Pineapple	52	50.3	96	18.3
		56.4	108	
		56.9	109	
GCE-PANI/CuOgrn Electrode				
Pineapple	52	42.3	85	12.7
		52.1	100	
		54.2	103	

CuOchm is more sensitive than GCE-PANI/CuOgrn, making it a suitable candidate for the detection of Trp.

Contributions

OEF conceptualized and designed the work and was part of the manuscript write-up. SJK, and AA were involved in the manuscript preparation. All the authors reviewed the manuscript and agreed to publication.

CRediT authorship contribution statement

Seleke J. Mokole: Data curation, Writing – original draft. **Ahmed Aliyu:** Visualization, Investigation, Writing – review & editing. **Omolola E. Fayemi:** Conceptualization, Methodology, Software, Supervision, Validation, Writing – review & editing.

Declaration of competing interest

The authors declare that they have no known competing financial interests or personal relationships that could have appeared to influence the work reported in this paper.

Acknowledgements

CEO, SAA, and OEF thank the North-West University and MaSIM for their financial support and research facilities. OEF acknowledges the FRC of North-West University and the National Research Foundation of South Africa for Thuthuka funding for Researchers (UID: 117709).

References

[1] R. Sundaresan, V. Mariyappan, S.M. Chen, M. Keerthi, R. Ramachandran, Electrochemical sensor for detection of tryptophan in the milk sample based on MnWO4 nanoplates encapsulated RGO nanocomposite, Colloids Surf. A 625 (2021) 126889.
[2] R.N. Goyal, S. Bishnoi, H. Chasta, M.A. Aziz, M. Oyema, Effect of surface modification of indium tin oxide by nanoparticles on the electrochemical determination of tryptophan, Talanta 85 (2011) 2626–2631.
[3] G.M. Brown, Light, melatonin and the sleep-wake cycle, J. Psychiatry Neurosci. 19 (1994) 345–353.
[4] Z. Tavokolian-Ardakani, O. Hosu, C. Cristea, M. Mazloum-Ardakani, G. Marrazza, Latest trends in electrochemical sensors for neurotransmitters: A, Review, Sens 19 (2019) 2037.
[5] F.J.V. Gomez, A. Martin, A. Escarpa, M.F. Silva, Screen-printed electrodes modified with carbon nanotubes or graphene for simultaneous determination of melatonin and serotonin, Microchim. Acta 182 (2015) 1925–1931.
[6] Q. He, Y. Tian, Y. Wu, J. Liu, G. Li, P. Deng, D. Chen, Electrochemical sensor for rapid and sensitive detection of tryptophan by a Cu2O nanoparticles-coated reduced graphene oxide nanocomposite, Biomolecules 9 (2019) 176.
[7] H. Li, Y. Wang, D. Ye, J. Luo, B. Su, S. Zhang, J. Kong, An electrochemical sensor for simultaneous determination of ascorbic acid, dopamine, uric acid and tryptophan based on MWNTs bridged mesocellular graphene foam nanocomposite, Talanta 127 (2014) 255–261.
[8] W. Prongmanee, I. Alam, P. Asanithi, Hydroxyapatite/Graphene oxide composite for electrochemical detection of L-Tryptophan, J. Taiwan Inst. Chem. Eng. 102 (2019) 415–423.
[9] L. Zhang, M. Sun, T. Jing, S. Li, H. Ma, A facile electrochemical sensor based on green synthesis of Cs/Ce-MOF for detection of tryptophan in human serum, Colloids Surf. A 648 (2022) 129225.
[10] S. Hasan, Review on nanoparticles: their synthesis and types, Res. J. Recent Sci. 4 (2015) 1–4.
[11] S. Taheriniya, Z. Behboodi, Comparing green chemical methods and chemical methods for the synthesis of titanium dioxide nanoparticles, Int. J. Pharm. Sci. Res. 7 (2016) 4927–4932.
[12] I. Ijaz, E. Gilani, A. Nazir, A. Bukhari, Detail review on chemical, physical and green synthesis, classification, characterizations and applications of nanoparticles, Green Chem. Lett. Rev. 13 (2020) 223–245.
[13] N. Kumar, S. Kumbhat, Essentials in Nanoscience and Nanotechnology, John Wiley & Sons, 2016.
[14] N. Maruthi, M. Faisal, N. Raghavendra, B.P. Prasanna, S.R. Manohara, M. Revanasiddappa, Anticorrosive polyaniline-coated copper oxide (PANI/CuO) nanocomposites with tunable electrical properties for broadband electromagnetic interference shielding, Colloids Surf. A: Physicochem. Eng. Asp. 621 (2021) 126611.
[15] S.P. Ashokkumar, H. Vijeth, L. Yesappa, M. Niranjana, M. Vandana, H. Devendrappa, Electrochemically synthesized polyaniline/copper oxide nano composites: To study optical band gap and electrochemical performance for energy storage devices, Inorg. Chem. Commun. 115 (2020) 107865.
[16] S.J. Mokole, A. Aliyu, O.E. Fayemi, Electrochemical detection of dopamine using green and chemical synthesized CuO/PANI nanocomposite modified electrode, Appl. Phys. A 129 (2023) 148.

[17] M.W. Ahmad, S. Anand, A. Fatima, D.J. Yang, A. Choudhury, Facile synthesis of copper oxide nanoparticles-decorated polyaniline nanofibers with enhanced electrochemical performance as supercapacitor electrode, Polym. Adv. Technol. 32 (2021) 4070–4081.
[18] J. Singh, G. Kaur, M. Rawat, A brief review on synthesis and characterization of copper oxide nanoparticles and its applications, J. Bioelectron. Nanotechnol. 1 (2016) 9.
[19] A.B.G. Trabelsi, A.M. Mostafa, F.H. Alkallas, W.B. Elsharkawy, A.N. Al-Ahmadi, H.A Ahmed, S.S. Nafee, R.A. Pashameah, E.A. Mwafy, Effect of CuO nanoparticles on the optical, structural, and electrical properties in the PMMA/PVDF nanocomposite, Micromachines 14 (6) (2023) 1195.
[20] M. Beygisangchin, S. Abdul Rashid, S. Shafie, A.R. Sadrolhosseini, H.N. Lim, Preparations, properties, and applications of polyaniline and polyaniline thin films-A review, Polymers 13 (12) (2021) 2003.
[21] J. Li, J. Jiang, Z. Xu, M. Liu, S. Tang, C. Yang, D. Qian, Pd-Cu@Cu_2O/N-RGO hybrid and its application for electrochemical detection of tryptophan, Electrochim. Acta 260 (2018) 526–535.
[22] S. Szunerits, Y. Coffinier, E. Galopin, J. Brenner, R. Boukherroub, Preparation of boron-doped diamond nanowires and their application for sensitive electrochemical detection of tryptophan, Electrochem. Commun. 12 (3) (2010) 438–441.
[23] J.V. Kumar, R. Karthik, S.M. Chen, S. Marikkani, A. Elangovan, V. Muthuraj, Green synthesis of a novel flower-like cerium vanadate microstructure for electrochemical detection of tryptophan in food and biological samples, J. Colloid Interface Sci. 496 (2017) 78–86.
[24] S. Naz, A. Gul, M. Zia, Toxicity of copper oxide nanoparticles: a review study, IET Nanotechnol 14 (2020) 1–13.
[25] S. Bellmaine, A. Schnellbaecher, A. Zimmer, Reactivity and degradation products of tryptophan in solution and proteins, Free Radic, Biol. M. 160 (2020) 696–718.
[26] J. Haywood, O. Mozziconacci, K.M. Allerge, B.A. Kerwin, C. Schoneich, Light- induced conversion of Trp to Gly and Gly hydroperoxide in IgG1, Mol. Pharm. 10 (3) (2013) 1146–1150.
[27] Q. Hao, W. Lei, X. Xia, Z. Yan, L. Lu, X. Wang, Exchange of counter anions in electropolymerized polyaniline films, Electrochim. Acta 55 (3) (2010) 632–640.
[28] D. Gizinski, A. Brudzisz, J.S Santos, F. Trivinho-Strixino, W.J. Stępniowski, T. Czujko, Nanostructured anodic copper oxides as catalysts in electrochemical and photoelectrochemical reactions, Catalysts 10 (11) (2020) 1338.
[29] A. Zestos, H. Chen, Effect of surface roughness on electrochemical adsorption/desorption of dopamine by carbonaceous electrodes, 2020.
[30] S.A. Balogun, O.E. Fayemi, Effects of electrolytes on the electrochemical impedance properties of NiPcMWCNTs-modified glassy carbon electrode, Nanomaterials 12 (11) (2022) 1876.
[31] S.D. GunaVuthana, J. Wilson, R. Prashnthi, A.C. Peter, CuO nanoflakes anchored polythiophene nanocomposite: Voltammetric detection of L-Tryptophan, Inorg. Chem. Commun. 124 (2021) 108398.
[32] F. Fazl, M.B. Gholivand, High performance electrochemical method for simultaneous detection of dopamine, serotonin, and tryptophan by ZrO_2-CuO co-doped CeO_2 modified carbon paste electrode, Talanta 239 (2022) 122982.
[33] R. Sundaresan, V. Mariyappan, S.M. Chen, M. Keerthi, R. Ramachandran, Electrochemical sensor for detection of tryptophan in milk sample based on $MnWO_4$ nanoplates encapsulated RGO nanocomposite, Colloids Surf. A Physiochem. Eng. Asp. 625 (2021) 126889.
[34] W. Huang, Y. Chen, L. Wu, M. Long, Z. Lin, Q. Su, F. Zheng, S. Wu, H. Li, G. Yu, 3D Co-doped Ni-based conductive MOFs modified electrochemical sensor for highly sensitive detection of l-tryptophan, Talanta 247 (2022) 123596.
[35] Z.Z. Tasic, M.B.P. Mihajlovic, M.B. Radovanovic, A.T. Simonovic, D.V. Medic, M.M. Antonijevic, Electrochemical determination of L-tryptophan in food samples on graphite electrode prepared from waste batteries, Sci. Rep. 12 (1) (2022) 5469.
[36] L. Zhang, M. Sun, M. Jing, T. Li, H. Ma, A facile electrochemical sensor based on green synthesis of Cs/Ce-MOF for detection of tryptophan in human serum, Colloids Surfaces A 648 (2022) 129225.
[37] S. Zhang, P. Ling, Y. Chen, J. Liu, C. Yang, 2D/2D porous Co_3O_4/rGO nanosheets act as an electrochemical sensor for voltametric tryptophan detection, Diam. Relat. Mater. 135 (2023) 109811.
[38] H. Meskher, F. Achi, H. Belkhalfa, Synthesis and characterization of CuO@PANI composite: A new prospective material for electrochemical sensing, J. Composit. Compounds 4 (13) (2022) 178–181.
[39] P.C. Motsaathebe, O.E. Fayemi, Serotonin electrochemical detection in tomatoes at MWCNT-AONP nanocomposite modified electrode, Mater. Res. Express 8 (2021) 115004.
[40] S. Romanowski, and L. Wojtczak, Electrode Surface Roughness, in Green Functions in Electrochemistry, S. Romanowski and L. Wojtczak, Editors. Springer Netherlands: Dordrecht. (1997) 217–249.
[41] S.K. Kim, I.J. Park, D.Y. Lee, Influence of surface roughness on the electrochemical behaviour of carbon steel, J. Appl. Electrochem. 43 (2013) 507–524.
[42] Y. Liu, L. Wang, L. Yang, A superior sensor for the electrochemical detection of Tryptophan in food samples using Ag-doped TiO2 nanoparticles modified glassy carbon electrode, Int. J. Electrochem. Sci. 16 (2021) 210534.
[43] C. Chauhan, Contemporary voltammetric techniques and its application to pesticide analysis: A review, Proceedings 37 (2021) 3231–3240.
[44] D. Lima, C.A. Pessoa, K. Wohnrath, L.H. Marcolino-Junior, M.F. Bergamini, A feasible and efficient voltametric sensor based on electropolymerized L-arginine for the tactionon of L-tryptophan in dietary supplements, Microchem. J. 181 (2022) 107709.
[45] B. Kaur, B. Satpati, R. Srivastava, Synthesis of NiCo2O4/Nano-ZSM-5 nanocomposite material with enhanced electrochemical properties for the simultaneous determination of ascorbic acid, dopamine, uric acid and tryptophan, New J. Chem. 39 (2015) 1115–1124.
[46] G.A. Tig, Development of electrochemical sensor for detection of ascorbic acid, dopamine, uric acid and l-tryptophan based on Ag nanoparticles and poly(l-arginine)-graphene oxide composite, J. Electroanal. Chem. 807 (2017) 19–28.